ACS OMEGA

http://pubs.acs.org/journal/acsodf

Article

A Modified Solid–Liquid–Gas Phase Equation of State

Chaoping Mo, Guangdong Zhang,* Zhiwei Zhang, Daibo Yan, and Sen Yang

Cite This: *ACS Omega* 2022, 7, 9322–9332

Read Online

ACCESS | Metrics & More | Article Recommendations | Supporting Information

ABSTRACT: The solid–liquid–gas equation of state (SLV-EOS) is based on the initial cubic equation of state, the van der Waals equation. Since the van der Waals equation is not accurate enough to predict gas–liquid properties, SLV-EOS cannot better predict the gas–liquid properties of hydrocarbons in actual gas reservoirs. Therefore, a modified solid–liquid–gas unified equation of state was constructed inthis paper, which was developed using the material's actual critical compressibility factor Z_c. The minimum liquid-phase volume at the triple point is also introduced to limit the value of c in the equation, which effectively avoids the solution of Maxwell's equal-area rule in the solid–liquid transformation process. The model extends the classical Peng–Robinson equation of state for fluid-only (liquid and vapor) states. The predicted p-T and p-ρ phase transition diagrams are reported in this paper for methane, ethane, propane, carbon dioxide, hydrogen sulfide, and sulfur, and they are in good agreement with the experimental data. This methodology is suitable for any substance for which the density of the solid phase is higher than that of the liquid phase. Additionally, the modified SLV equation can be used to estimate the solubility of solid sulfur in the absence of relevant experimental data.

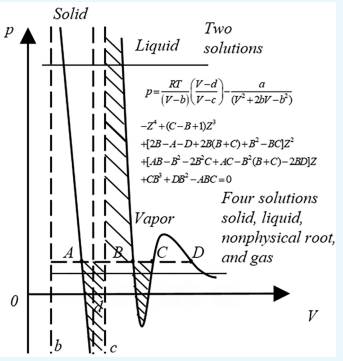

1. INTRODUCTION

Johanes Diderik van der Waals[1] first proposed the empirical equation of state describing the gas–liquid two-phase state. The equation as a whole consists of a combination of intermolecular repulsion p_{HC} and intermolecular mutual attraction p_A.

$$p = p_{HC} + p_A = \frac{RT}{V-b} - \frac{a}{V^2} \quad (1)$$

Since the famous van der Waals (vdW) equation of state (EOS) was established, many modified EOSs have been constructed to improve the accuracy of the description of the phase states. Lebowitz and Penrose[2] proved the phase change process of matter based on van der Waals. They improved the accuracy of the equation for predicting the thermodynamic properties of pure substances and mixtures. The most well-known modifications of the vdW EOS are the Soave–Redlich–Kwong (SRK) (Soave),[3] Peng–Robinson (PR) (Peng and Robinson),[4] and Patel-Teja (PT) (Patel and Teja)[5] EOSs. Many scholars have made numerous modifications to these equations, and these modifications to the PR EOS fall into four main categories:[6]

(1) Changing the correlation structure between α and the temperature or the expressions of the parameters a and b.
(2) Introducing a deviation function (like volume translation).
(3) Adding new parameters or terms to the state equation.
(4) Modifying the mixing rules for mixing applications.

However, vdW, SRK, and PR are two-parameter EOSs in which all compounds have the same critical compressibility factor, which leads to considerable bias in the prediction of liquid density. Bian[7] improved the prediction accuracy of the cubic EOS at the critical point by revising the critical compressibility factor Z_c. Abudour[8] proposed a new volume translation function for liquid mixture densities, which improved the prediction accuracy of the PR equation. Ghoderao[9] proposed a five-parameter cubic equation of state (5PGDN), which improved the prediction accuracy for pure substances. Still, the multiparameter equations do not produce significantly better predictions for mixtures, indicating the need for more complex mixing rules. However, the applicability of the 5PGDN proposed above is limited to gas and liquid phases. It does not provide an independent description of the physical properties of the solid phase, which often requires a combination of other thermal parameters.

In contrast, few studies have simultaneously considered the three-phase solid–liquid–gas phase transition. Wenzel[10] modified the gravitational term of the RK EOS to make it applicable to the solid–liquid turning point approach for pure components by calculating the volume-change characteristics of substances in the solid and liquid regions and describing the continuous phase changes of the gas, liquid, and solid as the substance changing with temperature and pressure. Salim[11] developed a modified TBS gas–solid equilibrium equation by regressing the gas and solid sublimation pressures below the triple point and using data on the enthalpy of evaporation and

Received: November 2, 2021
Accepted: March 2, 2022
Published: March 10, 2022

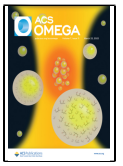

https://doi.org/10.1021/acsomega.1c06142
ACS Omega 2022, 7, 9322–9332

the isobaric heat capacity of the solid phase at the triple point. Yokozeki[12] introduced the discontinuity of the solid−liquid transition in the isothermal $p-V$ phase diagram of pure substances, avoiding the solid−liquid critical point, and proposed an analytic equation of state (SLV-EOS) considering the three solid−liquid−gas phases. Lee[13] pointed out that Yokozeki's equation modified the repulsive part of the EOS so that it had two singularities, one for the upper limit of the fluid region and the other for that of the solid region. This approach produces a discontinuous isotherm, implying a discontinuous variation of the phase transition and a repulsive term p_{HC} less than zero during the solid−liquid phase transition. In the same year, Lee[14] corrected the solid−liquid transition using extended Veytsman statistics and a lattice fluid model. The results were consistent with experimental data for the fluid phase but underestimated both the solid-phase density and the triple-point temperature. A critical point for the solid−liquid phase transition has not been confirmed in the currently known experimental data.

Furthermore, many scholars[15−17] have avoided the existence of the critical point in the solid−liquid phase transition process. Stringari[18] introduced the discontinuity of the solid−liquid transition in the SLV equation for CO_2, CH_4, C_2H_6, and C_3H_8, which were parametrically fitted to determine their SLV equation parameters. Still, the accuracy was not high when the liquid−solid nature was also considered. Marn-Garca[19] proposed a method for predicting solid−liquid, solid−gas, and liquid−gas coexistence using a noncubic equation of state, but the equations must be fitted to determine the seven parameters for each substance and the method is difficult to use.

Since the SLV-EOS established by Yokozeki is based on the van der Waals EOS equation, the SLV-EOS equation is not accurate enough to predict the gas−liquid properties of hydrocarbons in actual gas reservoirs. For example, the critical compressibility factor of substances in the van der Waals EOS equation is 0.375. For most substances, the value of 0.375 deviates too much from the critical compressibility factor of actual substances (generally 0.264−0.292). Thus, equations that can describe the physical properties of both the gas and the liquid more accurately should be considered. Therefore, this paper details the construction of a modified solid−liquid−gas unified equation of state, which was developed using the material's actual critical compressibility factor Z_c. A minimum liquid-phase volume at the triple point is also introduced to limit the value of c in the equation, which effectively avoids the solution of Maxwell's equal-area rule in the solid−liquid transformation process.

2. ESTABLISHMENT OF A MODIFIED SOLID−LIQUID−GAS UNIFIED EQUATION OF STATE

2.1. Development of the Model. The established solid−liquid−gas continuum equation of state should have a more robust applicability (expanding the EOS from gas−liquid two-phase state to the solid−liquid−gas three-phase state). At the same time, the form should conform to the corresponding thermodynamic conditions, which are summarized in the following points:

(1) The predicted gas- and liquid-phase properties should be consistent with the PR equation, and the phase change between the gas and liquid phasesshould be continuous. There is a critical point of the gas−liquid phase change that should be consistent with the form of the ideal gas equation of state.
(2) There should be a stable solid phase in a particular region where the gas and liquid phases exist in the phase diagram. The pressure change of the solid phase with volume should be similar to that of the liquid phase; considering the actual physical significance, there is no critical point of phase change between the solid and liquid phases.
(3) The prediction of thermodynamic properties, such as volume and density, of the solid phase at different pressures and temperatures can be consistent with the changing pattern of the actual substance; the solid−liquid−gas properties that change with pressure and temperature can be described.

The modified SLV EOS was established as follows (Figure 1):

$$p = \frac{RT}{(V-b)}\left(\frac{V-d}{V-c}\right) - \frac{a}{(V^2+2bV-b^2)} \quad (2)$$

where p is the pressure (MPa), T is the temperature (K), V is the volume (cm^3/mol), $R = 8.314472$ is the ideal gas constant, a is a parameter of the equation, b is the minimum volume of the solid (cm^3/mol), d is the maximum volume of the solid (cm^3/mol), and c is the minimum volume of the liquid (cm^3/mol).

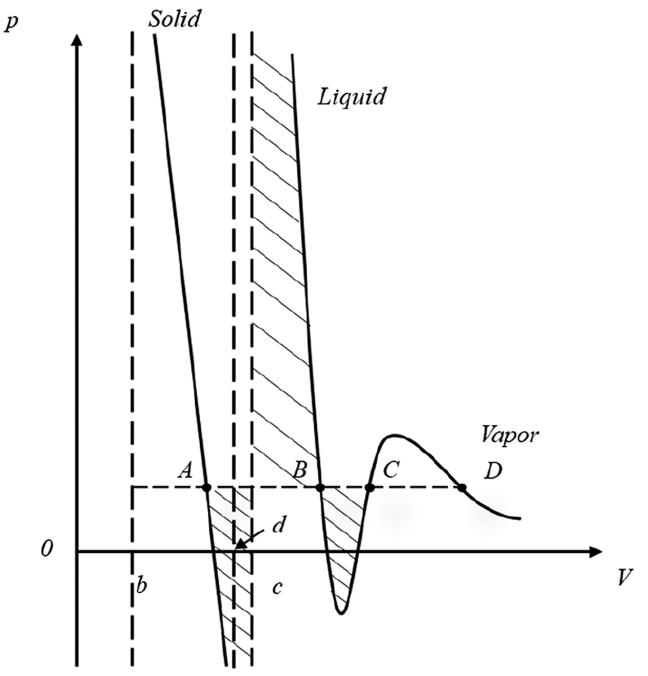

Figure 1. Schematic isothermal $p-V$ diagram of eq 2 at the solid−liquid−vapor triple point, where $0 < b < d < c$ and $V > b$.

In terms of dimensionless parameters, eq 2 can be rewritten as

$$p_r = \frac{T_r}{Z_c(V_r-b_r)}\left(\frac{V_r-d_r}{V_r-c_r}\right) - \frac{a_r}{Z_c^2(V_r^2+2b_rV_r-(b_r)^2)} \quad (3)$$

where the reduced parameters are defined as $Z_c = \frac{p_cV_c}{RT_c}$, $p_r = \frac{p}{p_c}$, $T_r = \frac{T}{T_c}$, $V_r = \frac{V}{V_c}$, $a_r = \frac{p_ca}{(RT_c)^2}$, $b_r = \frac{b}{V_c}$, $c_r = \frac{c}{V_c}$, and $d_r = \frac{d}{V_c}$.

The fugacity coefficient is expressed as

https://doi.org/10.1021/acsomega.1c06142
ACS Omega 2022, 7, 9322−9332

$$\ln\phi = \frac{1}{(b-c)}\left[c\ln\left|1-\frac{c}{V}\right| - b\ln\left|1-\frac{b}{V}\right| + d\ln\left|\frac{V-b}{V-c}\right|\right] - \frac{a}{RT2\sqrt{2}b}\ln\left|\frac{V+(1+\sqrt{2})b}{V+(1-\sqrt{2})b}\right| + Z - \ln Z - 1 \tag{4}$$

The reduced residual entropy is as follows:

$$\Delta S'/R = T_r\int_{\infty}^{V_r}\frac{(\partial Z/\partial T_r)_{V_r}}{V_r}dV_r + \int_{\infty}^{V_r}\frac{Z-1}{V_r}dV_r + \ln Z = \frac{1}{c_r-b_r}\left(c_r\ln\left|1-\frac{c_r}{V_r}\right| + d_r\ln\left|\frac{V_r-b_r}{V_r-c_r}\right| - b_r\ln\left|1-\frac{b_r}{V_r}\right|\right) + \frac{a_r}{T_rZ_c2\sqrt{2}b_r}\ln\left|\frac{V_r+(1+\sqrt{2})b_r}{V_r+(1-\sqrt{2})b_r}\right| + \frac{b_r-d_r}{V_r-b_r} + \frac{c_r-d_r}{V_r-c_r} + \left(\frac{da_r}{dT_r}-\frac{a_r}{T_r}\right)\frac{1}{2\sqrt{2}b_rZ_c}\ln\left|\frac{V_r+(1+\sqrt{2})b_r}{V_r+(1-\sqrt{2})b_r}\right| + \ln Z \tag{5}$$

The reduced residual enthalpy is as follows:

$$\Delta H'/RT_c = T_r^2\int_{\infty}^{V_r}\frac{(\partial Z/\partial T_r)_{V_r}}{V_r}dV_r + T_r(Z-1) = T_r\left(\frac{b_r-d_r}{V_r-b_r} + \frac{c_r-d_r}{V_r-c_r} + \left(\frac{da_r}{dT_r}-\frac{a_r}{T_r}\right)\frac{1}{2\sqrt{2}b_rZ_c}\ln\left|\frac{V_r+(1+\sqrt{2})b_r}{V_r+(1-\sqrt{2})b_r}\right|\right) + T_r(Z-1) \tag{6}$$

The reduced isochoric heat capacity is as follows:

$$\Delta C_v'/R = T_r\int_{\infty}^{V_r}\left(\frac{\partial^2 p_r}{\partial T_r^2}\right)_{V_r}dV_r = \frac{T_r}{2\sqrt{2}b_rZ_c}\ln\left|\frac{V_r+(1+\sqrt{2})b_r}{V_r+(1-\sqrt{2})b_r}\right|\left(\frac{d^2a_r}{dT_r^2}\right) \tag{7}$$

The coefficient of thermal expansion is as follows:

$$\alpha_p = \frac{1}{V}\left(\frac{\partial V}{\partial T}\right)_p \tag{8}$$

The isothermal bulk compressibility is as follows:

$$\beta_T = -\left(\frac{1}{V}\right)\left(\frac{\partial V}{\partial p}\right)_T \tag{9}$$

The isobaric heat capacity is as follows:

$$C_p = C_V + \frac{\alpha_p^2 TV}{\beta_T} \tag{10}$$

The speed of sound is as follows:

$$u^2 = \frac{C_p}{C_V}\frac{V}{M\beta_T} \tag{11}$$

The modified SLV (MSLV) EOS equation translates the compressibility factor Z into a quadratic equation that has four roots. The four roots present are ordered from smallest to largest in order of the compressibility factor of the solid phase, the compressibility factor of the liquid phase, the nonphysical roots of the gas−liquid equilibrium region, and the compressibility factor of the gas phase. The MSLV EOS uses the condition $b < d < c$, and the shaded part needs to satisfy Maxwell's equal-area rule for a solid−liquid−gas phase transition.

Combining this eq 2 with $pV = ZRT$, we obtain the following:

$$-Z^4 + (C-B+1)Z^3 + [2B - A - D + 2B(B+C) + B^2 - BC]Z^2 + [AB - B^2 - 2B^2C + AC - B^2(B+C) - 2BD]Z + CB^3 + DB^2 - ABC = 0 \tag{12}$$

where

$$A = \frac{ap}{(RT)^2},\ B = \frac{bp}{RT},\ C = \frac{cp}{RT},\ D = \frac{dp}{RT} \tag{13}$$

Solving eq 12 can yield Z_S, Z_L, and Z_V and bringing Z_S, Z_L, and Z_V into eq 4 can yield the solid, liquid, and gas fugacity coefficients.

2.2. Confirmation of Parameters. The MSLV-EOS equation includes four unknowns of a, b, c, and d. The equation needs to satisfy the gas−liquid two-phase equilibrium and the existence of solid-phase branches while solving the equation. The critical point needs to be satisfied when the equation exists in the gas−liquid two-phase equilibrium as follows:

$$p_{rc} = 1,\ T_{rc} = 1,\ V_{rc} = 1,\ \frac{\partial p_r}{\partial V_r} = 0,\ \frac{\partial^2 p_r}{\partial V_r} = 0 \tag{14}$$

where the subscript rc is the dimensionless value of the parameter at the critical point.

The first-order partial derivatives and second-order partial derivatives of the volume are obtained separately for the contrasted state form of the MSLV EOS as follows:

$$\frac{1}{Z_c(b_{rc}-V_{rc})(c_{rc}-V_{rc})} - \frac{T_{rc}(d_{rc}-V_{rc})}{Z_c(b_{rc}-V_{rc})(c_{rc}-V_{rc})^2} - \frac{T_{rc}(d_{rc}-V_{rc})}{Z_c(b_{rc}-V_{rc})^2(c_{rc}-V_{rc})} + \frac{a_{rc}(2b_{rc}+2V_{rc})}{Z_c^2(V_{rc}^2+2V_{rc}b_{rc}-b_{rc}^2)^2} = 0 \tag{15}$$

$$\frac{2a_{rc}}{Z_c^2(-b_{rc}^2+2V_{rc}b_{rc}+V_{rc}^2)^2} + \frac{2T_{rc}}{Z_c(b_{rc}-V_{rc})(c_{rc}-V_{rc})^2} + \frac{2T_{rc}}{Z_c(b_{rc}-V_{rc})^2(c_{rc}-V_{rc})} - \frac{2T_{rc}(d_{rc}-V_{rc})}{Z_c(b_{rc}-V_{rc})(c_{rc}-V_{rc})^3} - \frac{2T_{rc}(d_{rc}-V_{rc})}{Z_c(b_{rc}-V_{rc})^2(c_{rc}-V_{rc})^2} - \frac{2T_{rc}(d_{rc}-V_{rc})}{Z_c(b_{rc}-V_{rc})^3(c_{rc}-V_{rc})} - \frac{2a_{rc}(2b_{rc}+2V_{rc})^2}{Z_c^2(-b_{rc}^2+2V_{rc}b_{rc}+V_{rc}^2)^3} = 0 \tag{16}$$

Substituting the critical point condition yields

$$1 = \frac{1}{Z_c(1-b_{rc})}\left(\frac{1-d_{rc}}{1-c_{rc}}\right) - \frac{a_{rc}}{Z_c^2(1+2b_{rc}-b_{rc}^2)} \tag{17}$$

https://doi.org/10.1021/acsomega.1c06142
ACS Omega 2022, 7, 9322−9332

$$\frac{1}{Z_c(b_{rc}-1)(c_{rc}-1)} - \frac{(d_{rc}-1)}{Z_c(b_{rc}-1)(c_{rc}-1)^2} - \frac{(d_{rc}-1)}{Z_c(b_{rc}-1)^2(c_{rc}-1)} + \frac{a_{rc}(2b_{rc}+2)}{Z_c^2(-b_{rc}^2+2b_{rc}+1)^2} = 0 \quad (18)$$

$$\frac{2a_{rc}}{Z_c^2(-b_{rc}^2+2b_{rc}+1)^2} + \frac{2}{Z_c(b_{rc}-1)(c_{rc}-1)^2} + \frac{2}{Z_c(b_{rc}-1)^2(c_{rc}-1)} - \frac{2d_{rc}-2}{Z_c(b_{rc}-1)(c_{rc}-1)^3} - \frac{2d_{rc}-2}{Z_c(b_{rc}-1)^2(c_{rc}-1)^2} - \frac{2d_{rc}-2}{Z_c(b_{rc}-1)^3(c_{rc}-1)} - \frac{2a_{rc}(2b_{rc}+2)^2}{Z_c^2(-b_{rc}^2+2b_{rc}+1)^3} = 0 \quad (19)$$

The constraints of the MSLV-EOS equation are $b < d < c$. By analyzing the above constraints based on satisfying the gas−liquid phase equilibrium to be closer to the gas−liquid characteristics of the natural substance, Z_c is based on the actual critical compressibility factor of the substance. Taking methane as an example, $Z_c = 0.286$.

Three equations and four unknowns can be obtained using this method. At this point, the addition of the triple-point parameter can determine the liquid's minimum compression volume c and simplify the equation to three equations corresponding to three unknowns, which theoretically exist as analytical solutions.

For a unified equation of state that can also describe the solid phase, the liquid−solid equilibria at the triple-point temperature and the corresponding melting pressure should also be satisfied. In other words, the corresponding solid- and liquid-phase volumes should be consistent with the measured values as follows:

$$V_{rS}(T_{rt}, p_{rt}) = V_{rS}(T_{rt}, p_{rt})_{observe} \quad (20)$$

$$V_{rL}(T_{rt}, p_{rt}) = V_{rL}(T_{rt}, p_{rt})_{observe} \quad (21)$$

$$V_{rV}(T_{rt}, p_{rt}) = V_{rV}(T_{rt}, p_{rt})_{observe} \quad (22)$$

where p_{rt} is the triple-point pressure (dimensionless parameters); T_{rt} is the triple-point temperature (dimensionless parameter); and V_{rS}, V_{rL}, and V_{rV} are the volumes (dimensionless parameters) of the solid, liquid, and gas phases, respectively.

The equations do not necessarily satisfy eqs 20−22 simultaneously, such as the melting pressure and the solid-phase volume. Moreover, the liquid-phase volume of the substance at the triple point may not always be found entirely in the corresponding databases or experimental manuals. Therefore, eqs 17−19 are used as optimization objectives in the parameter solution. They ensure the correctness of the unified equation for predicting gas, liquid−solid, and physical properties at the critical point temperature.

So that each parameter of the critical point can accurately satisfy the gas−liquid critical point condition and the triple-point condition, the measured volume of the liquid phase at the triple point is used to limit the minimum volume of the material liquid phase that can be compressed, c_{rc}. In contrast, the universal global optimization (UGO) method is used to find the nested iterative sum of a_{rc}, b_{rc}, and d_{rc}. The flow of solving the essential parameters of the point is as follows (Figure 2):

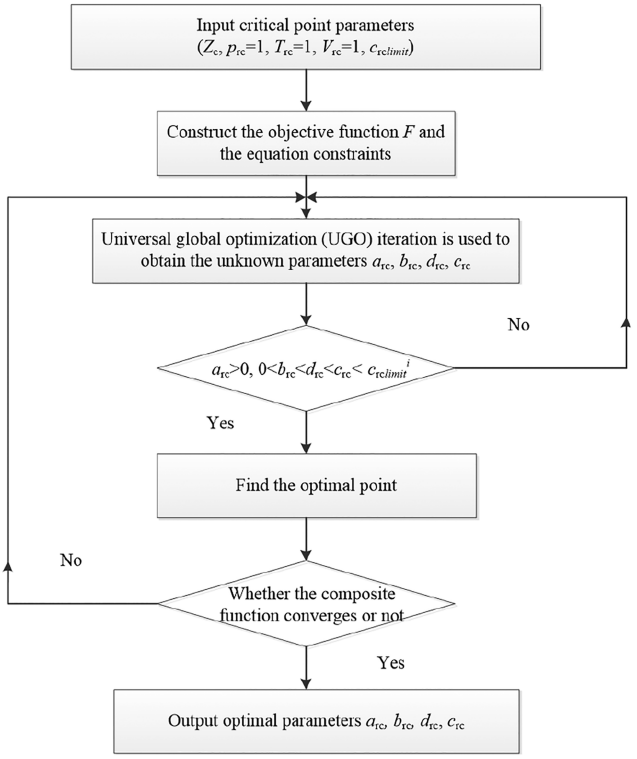

Figure 2. Parameter iteration flowchart.

(1) The critical point conditions for the input substance Z_c^i, $c_{rclimit}^i$, $p_{rc} = 1$, $V_{rc} = 1$, and $T_{rc} = 1$.
(2) Use eqs 20−22 as a constraint range while satisfying $b^i < d^i < c^i$.
(3) Iterate eqs 17−19 using the UGO method to find the corresponding parameters.
(4) For each set of parameters found, determine whether they satisfy $a_{rc}{}^i > 0$, $0 < b_{rc}{}^i < d_{rc}{}^i < c_{rc}{}^i < c_{rclimit}{}^i$. If yes, proceed to the next step. If no, return to step 3.
(5) Find the optimal point of the composite objective function.
(6) Determine whether the objective function converges or not, and return to step 3 if it does not. If it converges, output the optimal parameter values under the objective function.

The parameters in the equation are expressed as functions of temperature, which can have better applicability. After repeated attempts, the expression form for the parameters of the equation was finally determined.

For a_r, the variational form in the original PR equation can still be followed.

$$a_r = a_{rc}\cdot\alpha(T_r) \quad (23)$$

$$\alpha(T_r) = [1 + m(1 - T_r^{0.5})]^2 \quad (24)$$

When $\omega < 0.491$,

$$m = 0.37464 + 1.54226\omega - 0.26992\omega^2 \quad (25)$$

When $\omega > 0.491$,

$$m = 0.374642 + 1.48504\omega - 0.164423\omega^2 + 0.016666\omega^3 \quad (26)$$

Ignoring the increase in temperature, the volume boundaries of the liquid and solid phases are constantly leaning in (with

https://doi.org/10.1021/acsomega.1c06142
ACS Omega 2022, 7, 9322−9332

Table 1. Parameters of Each Pure Compound[20,22−30]

	p_c (MPa)	T_c, (K)	ω	Z_c	V_c (cm^3/mol)	p_t (MPa)	T_t (K)
CH_4	4.599	190.56	0.011	0.286	98.6	0.011692	90.3941
C_2H_6	4.872	305.32	0.099	0.279	145.5	1.14×10^{-06}	90.368
C_3H_8	4.248	369.83	0.152	0.276	200	1.7×10^{-10}	85.525
CO_2	7.374	304.12	0.225	0.274	94.07	0.51795	216.592
H_2S	8.963	373.4	0.09	0.283	98	0.0222748	187.68
S_8	5.2	1065	0.3805	0.1634	278.2738	2.3998×10^{-06}	387.65

minor changes). The distances between d_r, b_r, and c_r are assumed to be constant to ensure that the phase change between the liquid and solid phases does not appear as a critical point, which is consistent with the liquid−solid phase change characteristics of the actual substance.

b_r, c_r, and d_r can be simplified as

$$b_r = b_{rc},\ c_r = c_{rc},\ d_r = d_{rc} \tag{27}$$

When each contrasting parameter in the equation is determined, each parameter of the equation in the original noncontrasting form can be found as follows:

$$a = a_r \frac{(RT_c)^2}{P_c},\ b = V_c b_{rc},\ c = V_c c_{rc},\ d = V_c d_{rc} \tag{28}$$

3. PURE COMPONENTS: CH_4, C_2H_6, C_3H_8, CO_2, H_2S, AND S_8

3.1. Fluid Component Parameters. This section will verify the feasibility of the proposed MSLV EOS equation by simulating the actual substance using the MSLV EOS equation. The triple point data of the substance and the critical point parameters were used to determine the parameters related to the substance for the constraints b, c, and d. The specific data are listed in Table 1.

With the method proposed in Section 2, it is possible to identify the parameters associated with the substances a, b, c, and d. Although they are not necessarily unique or optimal, the set of parameters obtained for CH_4, C_2H_6, C_3H_8, CO_2, H_2S, and S_8 are listed in Table 2. EOS parameters have been established to predict various thermodynamic properties and the phase behavior of these compounds.

Table 2. EOS Constants for a_{rc}, b_{rc}, d_{rc}, and c_{rc}

	a_{rc}	b_{rc}	d_{rc}	c_{rc}
CH_4	0.4902264	0.2989634	0.3603434	0.3604034
C_2H_6	0.4795142	0.2970187	0.3171974	0.3171983
C_3H_8	0.4741352	0.2950876	0.3006134	0.3007413
CO_2	0.4527902	0.2790526	0.3965235	0.3969935
H_2S	0.4801457	0.2923996	0.3519409	0.3520109
S_8	0. 4284803	0.4250416	0.4888738	0.5098754

The number after the decimal point in Table 2 can be reduced appropriately. However, the values of d_{rc} and c_{rc} are very close to each other, and it is necessary to ensure that $d_{rc} < c_{rc}$ while choosing a valid number.

3.2. Phase Diagram of Each Component. To facilitate the comparison between the predicted results of the MSLV equation and the experimental values, the $p-T$ phase diagrams for each component of the anticipated results and the saturated fluid density curve for each element were plotted.

The reference for the uncertainty estimation is the EURACHEM/CITAC guide *Quantifying Uncertainty in Analytical Measurement*.[21]

The total uncertainties of the vapor pressure, sublimation pressure, and melting pressure predictions (Figure 3) were estimated to be 0.620%, 0.00032%, and 0.0226%, respectively (coverage factor $k = 2$ corresponding to a level of confidence of about 95%).

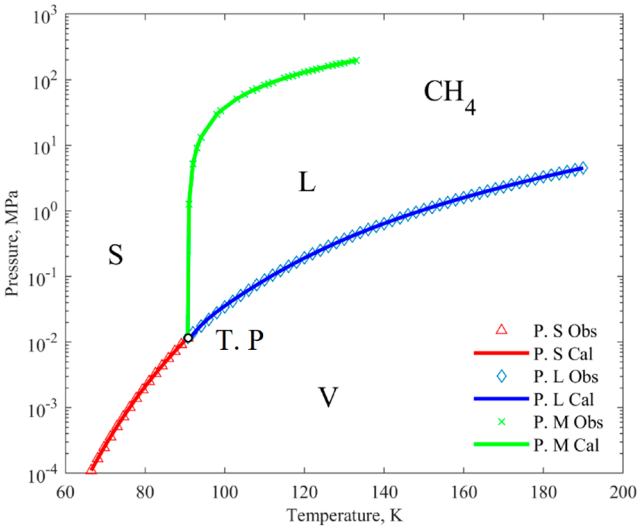

Figure 3. Phase diagram of CH_4 in the $p-T$ projection. Lines were calculated with the present EOS. Symbols represent selected experimental data.[20] T. P is the triple point, Obs the is literature value, Cal is the model prediction value, P. S is the sublimation pressure, P. L is the vapor pressure, and P. M is the melting pressure.

The total uncertainties of the vapor pressure, sublimation pressure, and melting pressure predictions (Figure 4) were estimated to be 0.481%, 0.0547%, and 0.0653%, respectively (coverage factor $k = 2$ corresponding to a level of confidence of about 95%).

The total uncertainties of the vapor pressure, sublimation pressure, and melting pressure predictions (Figure 5) were estimated to be 1.510%, 9.025%, and 0.00362%, respectively (coverage factor $k = 2$ corresponding to a level of confidence of about 95%).

The total uncertainties of the vapor pressure, sublimation pressure, and melting pressure predictions (Figure 6) were estimated to be 0.0147%, 9.102%, and 1.68%, respectively (coverage factor $k = 2$ corresponding to a level of confidence of about 95%).

The total uncertainties of the vapor pressure, sublimation pressure, and melting pressure predictions (Figure 7) were estimated to be 0.714%, 8.625%, and 1.165%, respectively (coverage factor $k = 2$ corresponding to a level of confidence of about 95%).

https://doi.org/10.1021/acsomega.1c06142
ACS Omega 2022, 7, 9322−9332

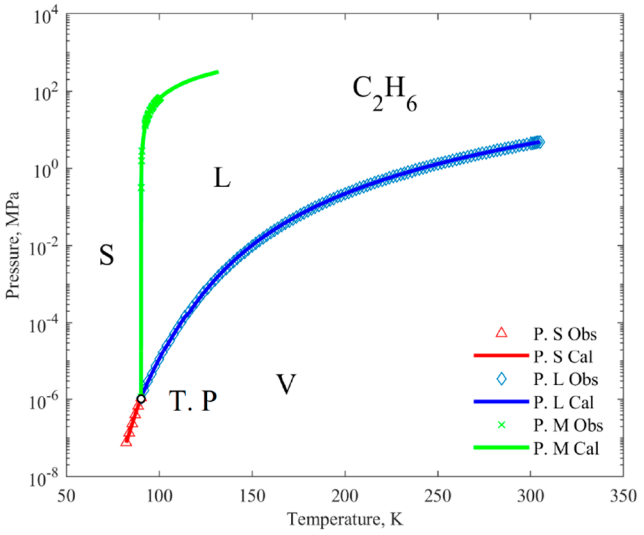

Figure 4. Phase diagram of C_2H_6 in the $p-T$ projection. Lines were calculated with the present EOS. Symbols represent selected experimental data.[22] T. P is the triple point, Obs is the literature value, Cal is the model prediction value, P. S is the sublimation pressure, P. L is the vapor pressure, and P. M is the melting pressure.

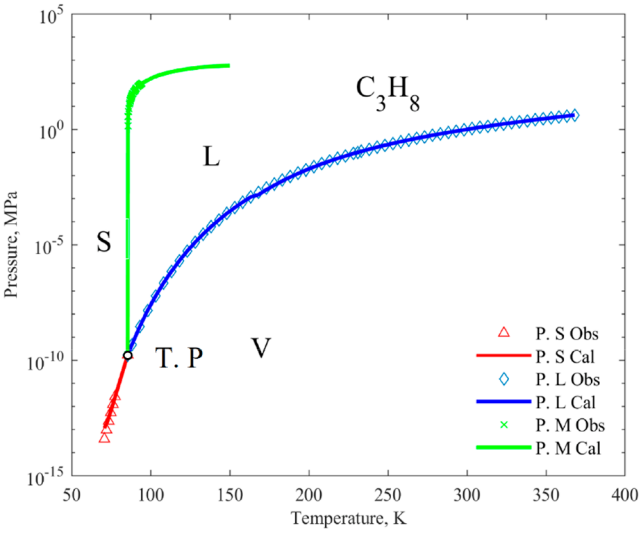

Figure 5. Phase diagram of C_3H_8 in the $p-T$ projection. Lines were calculated with the present EOS. Symbols represent selected experimental data.[23,24] T. P is the triple point, Obs is the literature value, Cal is the model prediction value, P. S is the sublimation pressure, P. L is the vapor pressure, and P. M is the melting pressure.

The total uncertainties of the vapor pressure and melting pressure predictions (Figure 8) were estimated to be 3.956% and 1.929%, respectively (coverage factor k = 2 corresponding to a level of confidence of about 95%).

The total uncertainties of the liquid, gas, and solid density predictions (Figure 9) were estimated to be 2.473%, 2.774%, and 0.361%, respectively (coverage factor k = 2 corresponding to a level of confidence of about 95%).

The total uncertainties of the liquid, gas, and solid density predictions (Figure 10) were estimated to be 1.405%, 2.177%, and 0.157%, respectively (coverage factor k = 2 corresponding to a level of confidence of about 95%).

The total uncertainties of the liquid, gas, and solid density predictions (Figure 11) were estimated to be 1.427%, 1.564%,

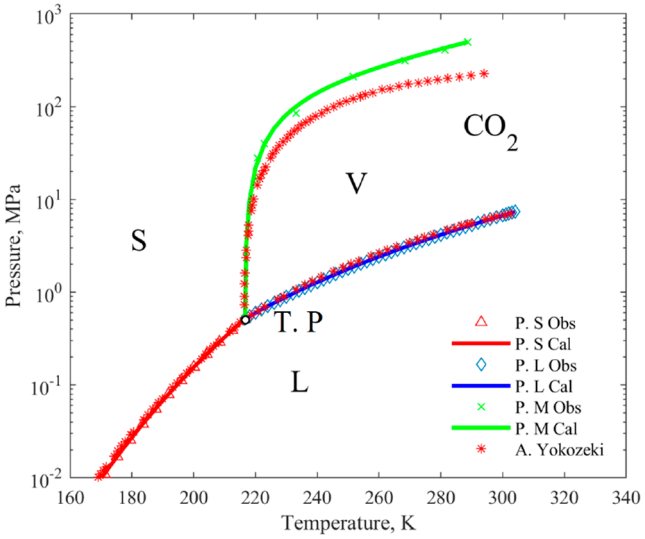

Figure 6. Phase diagram of CO_2 in the p-T projection. Lines: calculated with the present EOS. Symbols: selected experimental data.[25] The T. P is the triple point, Obs is the literature value, Cal is the model prediction value, P. S is the sublimation pressure, P. L is the vapor pressure, and P. M is the melting pressure.

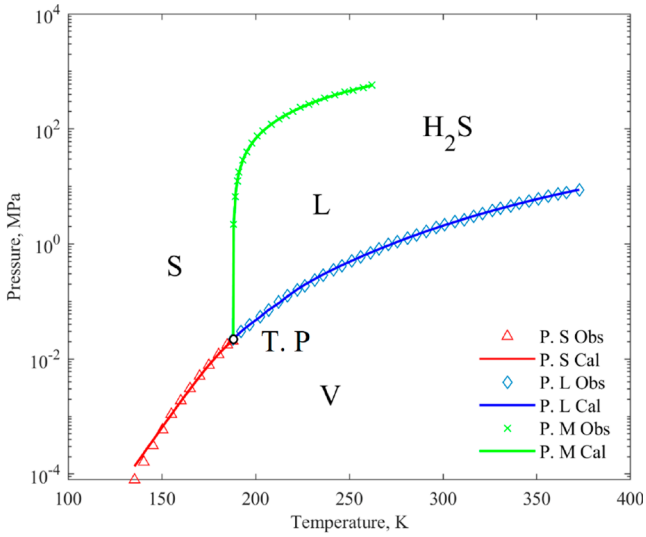

Figure 7. Phase diagram of H_2S in the $p-T$ projection. Lines were calculated with the present EOS. Symbols represent selected experimental data.[26,27] T. P is the triple point, Obs is the literature value, Cal is the model prediction value, P. S is the sublimation pressure, P. L is the vapor pressure, and P. M is the melting pressure.

and 0.251%, respectively (coverage factor k = 2 corresponding to a level of confidence of about 95%).

The total uncertainties of the liquid and gas density predictions (Figure 12) were estimated to be 1.216% and 1.206%, respectively (coverage factor k = 2 corresponding to a level of confidence of about 95%).

The total uncertainties of the liquid and solid density predictions (Figure 13) were estimated to be 0.899% and 5.878%, respectively (coverage factor k = 2 corresponding to a level of confidence of about 95%).

The total uncertainty of the liquid density predictions (Figure 14) was estimated to be 1.192% (coverage factor k = 2 corresponding to a level of confidence of about 95%).

https://doi.org/10.1021/acsomega.1c06142
ACS Omega 2022, 7, 9322−9332

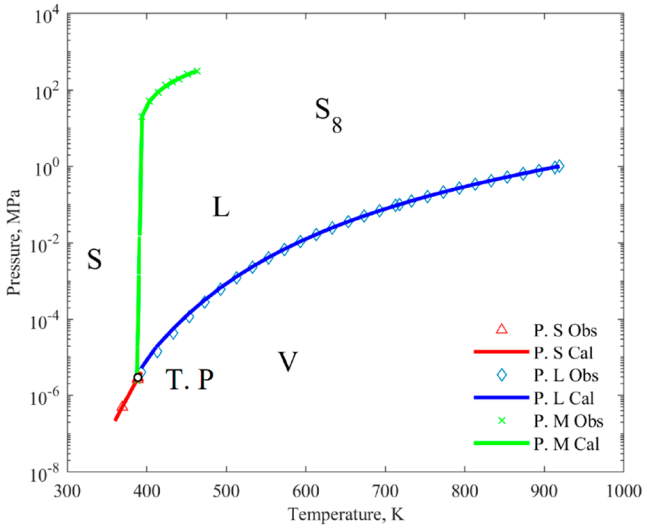

Figure 8. Phase diagram of S_8 in the $p-T$ projection. Lines were calculated with the present EOS. Symbols represent selected experimental data.[28−30] T. P is the triple point, Obs is the literature value, Cal is the model prediction value, P. S is the sublimation pressure, P. L is the vapor pressure, and P. M is the melting pressure.

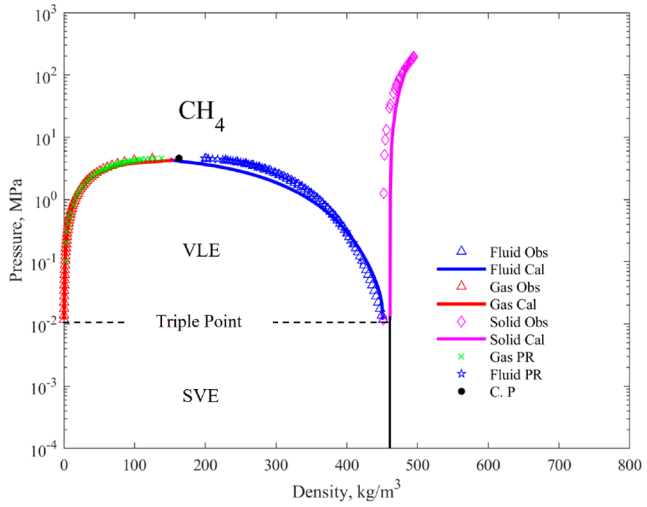

Figure 9. Phase diagram of CH_4 in the $p-\rho$ projection. Lines were calculated with the present EOS. Symbols represent selected experimental data.[20] C. P is the critical point, Obs is the literature value, and Cal is the model prediction value.

4. CALCULATION OF THE SOLUBILITY OF SOLID SULFUR IN GAS MIXTURES

The current phase equilibrium models (PR, PR-BM, and SRK) are not applicable when one phase is a high-pressure gas and the other is a solid.[31] In solid−gas equilibrium, the thermodynamic conditions imply that the pressure, temperature, and fugacity of both phases are the same as follows:

$$f_i^{\mathrm{V}} = f_i^{\mathrm{S}} \tag{29}$$

The EOS can be used for calculations in the gas phase but not in the solid phase, so the solid−gas equilibrium equation needs to be converted to the following equation:

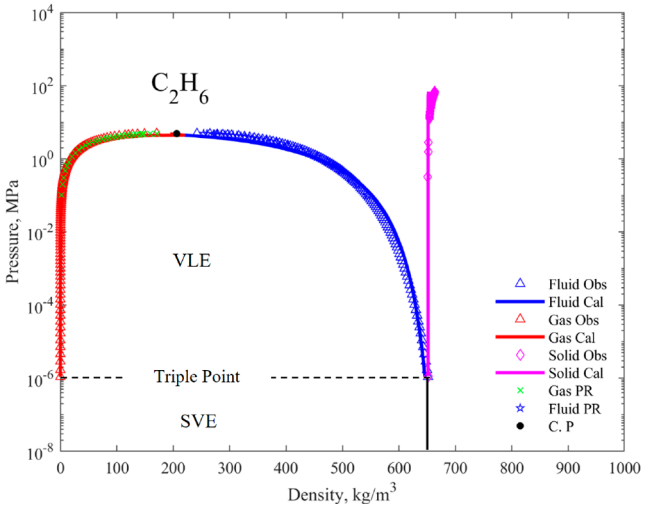

Figure 10. Phase diagram of C_2H_6 in the $p-\rho$ projection. Lines were calculated with the present EOS. Symbols represent selected experimental data.[22] The C. P is the critical point, Obs is the literature value, and Cal is the model prediction value.

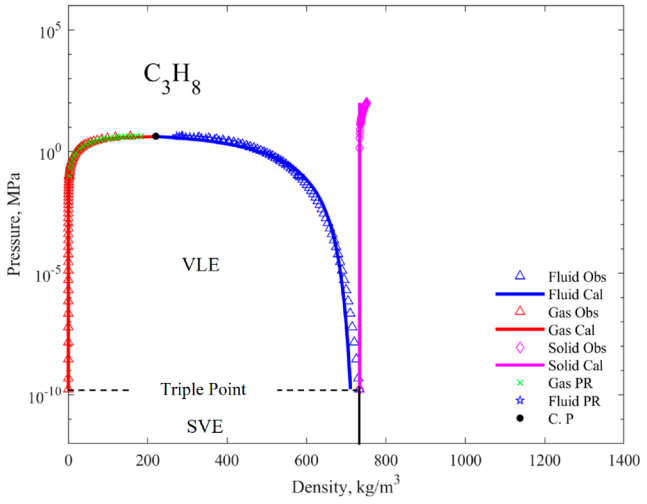

Figure 11. Phase diagram of C_3H_8 in the $p-\rho$ projection. Lines were calculated with the present EOS. Symbols represent selected experimental data.[23,24] C. P is the critical point, Obs is the literature value, and Cal is the model prediction value.

$$f_i^{\mathrm{V}} = y_1\phi_1^{\mathrm{V}}p = x_1^{\mathrm{S}}\gamma_1^{\mathrm{S}}\phi_1^{\mathrm{S}}p_1^{\mathrm{sub}}\exp\left(\int_{p_1^{\mathrm{sub}}}^{p}\frac{V_i^{\mathrm{S}}\mathrm{d}p}{RT}\right) = f_i^{\mathrm{S}} \tag{30}$$

where the superscript S refers to the solid phase and p_1^{sub} refers to the sublimation pressure (the equilibrium pressure when the pure component and its vapor fugacity are in equilibrium).

Assuming that the solid is a pure component and incompressible and that p_1^{sub} is much smaller than p, eq 30 can be transformed as follows:

$$y_1\phi_1^{\mathrm{V}}p = p_1^{\mathrm{sub}}\exp\left(\frac{V_i^{\mathrm{S}}p}{RT}\right) \tag{31}$$

The most crucial thing in eq 31 is to find y_1, which is usually small ($<10^{-3}$) for specific temperature and pressure conditions. The conventional approach assumes the density of the gas phase as the density of the pure gas component and uses the

https://doi.org/10.1021/acsomega.1c06142
ACS Omega 2022, 7, 9322−9332

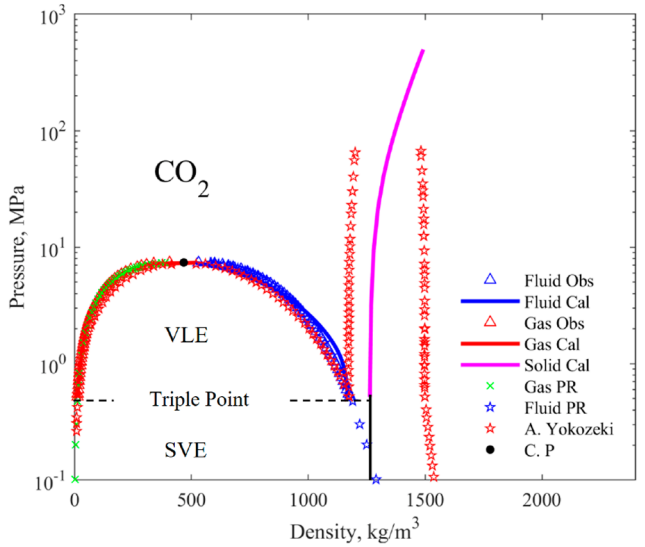

Figure 12. Phase diagram of CO_2 in the $p-\rho$ projection. Lines were calculated with the present EOS. Symbols represent selected experimental data.[25] The C. P is the critical point, Obs is the literature value, and Cal is the model prediction value.

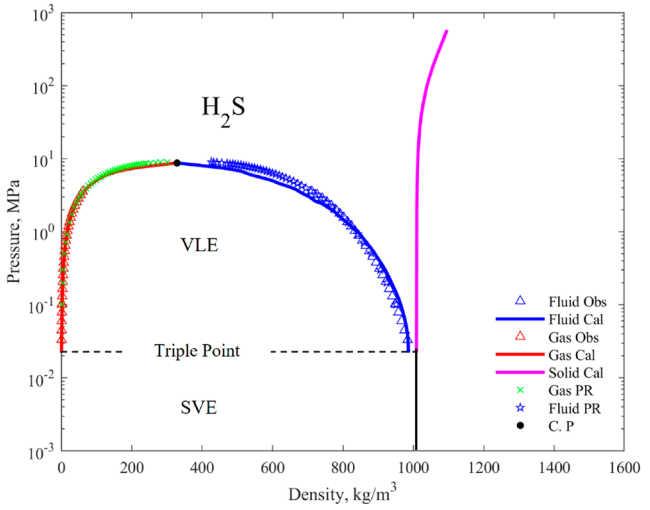

Figure 13. Phase diagram of H_2S in the $p-\rho$ projection. Lines were calculated with the present EOS. Symbols represent selected experimental data.[26,27] C. P is the critical point, Obs is the literature value, and Cal is the model prediction value.

correlation or estimation equation to find ϕ_1^V, p_1^{sub}, and V_i^S. Alternatively, by assuming p_1^{sub} and V_i^S data and using the EOS to find ϕ_1^V (commonly using the PR equation), the fugacity coefficient of S_8 in sour gas will be infinite, making it impossible to calculate, and the calculation of sublimation pressure will require the intervention of Antoine's equation. Therefore, this paper uses the MSLV equation to predict the solubility of solid sulfur in gas mixtures. The data used are shown in Table 3.[32]

Elemental sulfur in sulfur-containing systems is a complex mixture that exists in several forms, from S_8 to S_1, through chemical decomposition and coexists in equilibrium in both a gas and liquid fluids, as shown by the reaction equations in eqs 32 and 33. Heidemann[33] pointed out the isomeric conversion from S_8 to sulfur with increasing temperature. At the same time, hydrogen sulfide and S_8 react to form a complex reaction of polysulfide. Therefore, the dissolved S_8 in gas mixtures is

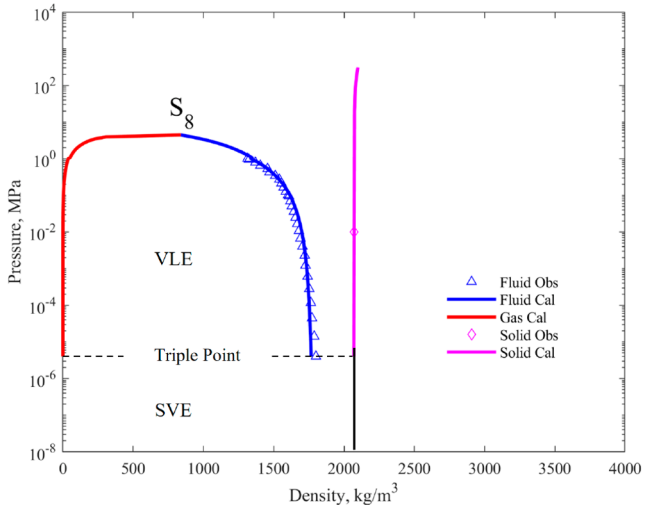

Figure 14. Phase diagram of S_8 in the $p-\rho$ projection. Lines were calculated with the present EOS. Symbols represent selected experimental data.[28−30] The C. P is the critical point, Obs is the literature value, and Cal is the model prediction value.

Table 3. Parameters of Each Component of the Sample[32]

component	mole fraction (%)
CH_4	73.418
C_2H_6	0.032
H_2S	17.891
CO_2	8.659

regarded as a complex mixture S_{8m}. The critical parameters of S_{8m} and the binary interaction coefficients of each component are shown in Tables 4 and 5, respectively.

$$\frac{m}{8}S_8 \rightleftharpoons S_m,\ m = 1, 2, 3, 4, 5, 6, 7 \tag{32}$$

$$H_2S + \frac{k-1}{8}S_8 = H_2S_k;\ k = 2, \ldots, 9 \tag{33}$$

Table 4. Parameters of S_{8m}

	p_c (MPa)	T_c (K)	ω
S_{8m}	5.406	1052	0.3805

We used a second-order polynomial to represent the methane−sulfur binary interaction parameter referenced from this literature.[34] In this paper, we have looked at sulfur as a pseudocomponent. Additionally, the binary interaction coefficients of methane and sulfur are viewed as a second-order

Table 5. Binary Interaction Parameters k_{ij} between CH_4, C_2H_6, H_2S, CO_2, and S_{8m} Molecules[a]

k_{ij}	CH_4	C_2H_6	H_2S	CO_2	S_{8m}
CH_4	0	−0.0026	0.08	0.0919	k_o
C_2H_6	−0.0026	0	0.0833	0.1322	0.1
H_2S	0.08	0.0833	0	0.097	0.0985
CO_2	0.0919	0.1322	0.097	0	0.165
S_{8m}	k_o	0.165	0.0985	0.1	0

[a] $k_o = -1.6716 \times 10^{-5}T^2 + 1.0002 \times 10^{-5}T - 1.2526$ $(T \leq 393.15K)$.

https://doi.org/10.1021/acsomega.1c06142
ACS Omega 2022, 7, 9322−9332

polynomial. We try to combine these two approaches to predict the solubility of sulfur in gas mixtures.

The fugacity of solid sulfur in gas mixtures and the fugacity of each gas component can be obtained from the mixture fugacity equation in the Appendix, and the solubility of solid sulfur in the sample gas can be obtained from eqs 34 and 35 to yield the data shown in Figure 15 and Table 6.

$$x_i = \frac{f_{S_8}^{S}}{f_{S_{8m}\text{mix}}^{V}} \tag{34}$$

$$c_{\text{Sulfur}} = \frac{256.528 x_n}{V_{\text{mix}}} \times 10^6 \tag{35}$$

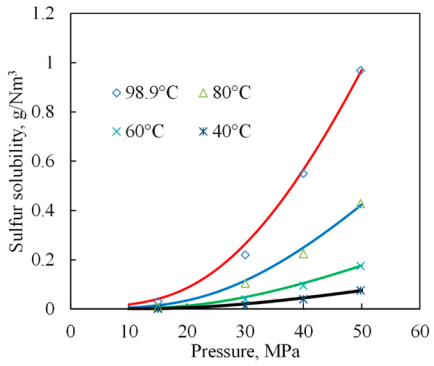

Figure 15. Comparison of the calculated solubility of solid sulfur with published data.[32] The symbols in the figure are the literature values, and the lines are the predicted result of the MSLV equation.

Table 6. Sulfur Solubility Data and Predicted Values at Different Temperatures and Pressures[32]

temperature (°C)	pressure (MPa)	measured value (g/Nm³)	predicted value (g/Nm³)	RD (%)
98.9	49.8	0.968	0.9612	−0.70
	40	0.55	0.566121	2.93
	30	0.22	0.26449	20.22
	15	0.031	0.041322	33.30
80	49.8	0.429	0.4206	−1.96
	40	0.225	0.249785	11.02
	30	0.104	0.11575	11.30
	15	0.008	0.015223	90.29
60	49.8	0.175	0.175216	0.12
	40	0.095	0.105153	10.69
	30	0.039	0.048609	24.64
	15	0.002	0.005205	160.24
40	49.8	0.076	0.074676	−1.74
	40	0.04	0.045378	13.45
	30	0.015	0.021154	41.03
	15	0.001	0.00185	84.99

The MSLV equation can predict the solubility of solid sulfur in gas mixtures. A total of 16 experimental values were compared, with an average relative deviation of 31.24%. The prediction accuracy is not satisfactory, especially for pressures below 30 MPa. However, in the absence of relevant experimental data (the Chrastil model and the Antoine equation for solid sulfur in gas mixtures cannot be fitted), the MSLV equation can be used as an alternative.

5. CONCLUSION

(1) A modified SLV equation of state is proposed to predict thermophysical properties such as vapor pressure, liquid density, vapor density, solid density, and the fugacity coefficient. The actual critical compressibility factor of the material is introduced in this equation to accurately predict the vapor−liquid physical properties of the material. The minimum liquid-phase volume at the triple point is also introduced to limit the value of c in the equation, which effectively avoids the solution of Maxwell's equal-area rule in the solid−liquid transformation process.

(2) The MSLV equation proposed in this paper, although a modified version of the SLV equation, does not solve the problem of the SLV equation having a negative value for p_{HC} at $b < V < c$. It only avoids the solution of Maxwell's equal-area rule by simplifying b, c, and d as constants rather than variables that vary with temperature.

(3) The $p-T$ and $p-\rho$ phase transition diagrams of methane, ethane, propane, carbon dioxide, hydrogen sulfide, and sulfur were reported to be predicted by the modified SLV equation, which agreed well with the literature data. Additionally, the predicted data were compared with the results of the PR equation and the Yokozeki model, showing the excellent prediction of the solid-phase volumes while ensuring the accuracy of the predictions for gas−liquid physical properties.

(4) In this paper, the solubility of solid sulfur in gas mixtures was predicted using the MSLV equation, and a total of 16 experimental values were compared and predicted with an average relative deviation of 31.24%. The prediction is not very accurate but at least shows that the proposed model can provide a rough estimate of solid solubility in gas mixtures without related experimental data.

APPENDIX A

When solving for the physical properties of a multivariate mixed system, the equation is shown as follow:

$$p = \frac{RT}{(V - b_m)}\left(\frac{V - d_m}{V - c_m}\right) - \frac{a_m}{(V^2 + 2b_m V - b_m^2)} \tag{A.1}$$

The mixture's equation parameters a_m, b_m, c_m, and d_m are obtained by employing the van der Waals and Lorentz−Berthelot mixing rule:

$$a_m = \sum_{i,j=1}^{N} \sqrt{a_i a_j}(1 - k_{ij}) x_i x_j \tag{A.2}$$

$$b_m = \sum_{i=1}^{N} b_i x_i,\ c_m = \sum_{i=1}^{N} c_i x_i,\ d_m = \sum_{i=1}^{N} d_i x_i \tag{A.3}$$

$$A = \frac{a_m p}{(RT)^2},\ B = \frac{b_m p}{RT},\ C = \frac{c_m p}{RT},\ D = \frac{d_m p}{RT} \tag{A.4}$$

$$p_{rc} = \frac{1}{Z_c(V_{rc} - b_{rc})}\left(\frac{V_{rc} - d_{rc}}{V_{rc} - c_{rc}}\right) - \frac{a_{rc}}{Z_c^2(V_{rc}^2 + 2b_{rc}V_{rc} - b_{rc}^2)} \tag{A.5}$$

The component fugacity coefficient in the mixture system is as follows:

https://doi.org/10.1021/acsomega.1c06142
ACS Omega 2022, 7, 9322−9332

$$\ln \phi_i = \frac{1}{b_m - c_m}\left[c_m \ln\left|1 - \frac{c_m}{V}\right| - b_m \ln\left|1 - \frac{b_m}{V}\right|\right] - \frac{c_i(b_m - d_m) + b_i(d_m - c_m) + (b_m - c_m)(d_m - d_i)}{(b_m - c_m)^2}\ln\left|\frac{V - c_m}{V - b_m}\right| - \frac{1}{b_m - c_m}\left[\frac{c_i(c_m - d_m)}{V - c_m} + \frac{b_i(d_m - b_m)}{V - b_m}\right] - \frac{a_m}{RTb_m}\frac{b_i V}{V^2 + 2b_m V - {b_m}^2} - \frac{a_m}{RT2\sqrt{2}b_m}\left(\frac{2\sum_{j=1}^{N}\sqrt{a_i a_j}(1 - k_{ij})x_j}{a_m} - \frac{b_i}{b_m}\right)\ln\left|\frac{V + (1 + \sqrt{2})b_m}{V + (1 - \sqrt{2})b_m}\right| - \ln Z \quad (A.6)$$

■ ASSOCIATED CONTENT

Supporting Information

The Supporting Information is available free of charge at https://pubs.acs.org/doi/10.1021/acsomega.1c06142.

Percentage deviation of calculated MSLV EOS values from literature density datas and density values calculated by the MSLV EOS (PDF)

■ AUTHOR INFORMATION

Corresponding Author

Guangdong Zhang − *Petroleum Engineering School, Southwest Petroleum University, Chengdu 610500, China*; Email: 510012301@qq.com

Authors

Chaoping Mo − *Petroleum Engineering School, Southwest Petroleum University, Chengdu 610500, China*; orcid.org/0000-0002-7726-9097

Zhiwei Zhang − *Petroleum Engineering School, Southwest Petroleum University, Chengdu 610500, China*

Daibo Yan − *Petroleum Engineering School, Southwest Petroleum University, Chengdu 610500, China*

Sen Yang − *Petroleum Engineering School, Southwest Petroleum University, Chengdu 610500, China*

Complete contact information is available at: https://pubs.acs.org/10.1021/acsomega.1c06142

Author Contributions

The manuscript was written through contributions of all authors. All authors have given approval to the final version of the manuscript.

Notes

The authors declare no competing financial interest.

■ ACKNOWLEDGMENTS

The study was supported by the National Natural Science Foundation of China (U19B6003).

■ ABBREVIATIONS:

5PGDN, five-parameter cubic equation of state; EOS, equation of state; RK, Redlich−Kwong; PR, Peng−Robinson; PT, Patel and Teja; SLV, solid−liquid−gas; SRK, Soave−Redlich−Kwong; TBS, Trebble-Bishnoi-Salim; vdW, van der Waals

■ REFERENCES

(1) Visser, J. Van der Waals and other cohesive forces affecting powder fluidization. *Powder Technol.* **1989**, *58* (1), 1−10.

(2) Lebowitz, J. L.; Penrose, O. Rigorous treatment of the Van Der Waals-Maxwell theory of the liquid-vapor transition. *Journal of Mathematical Physics* **1966**, *7* (1), 98−113.

(3) Soave, G. Equilibrium constants from a modified Redlich-Kwong equation of state. *Chemical engineering science* **1972**, *27* (6), 1197−1203.

(4) Peng, D.-Y.; Robinson, D. B. A new two-constant equation of state. *Industrial & Engineering Chemistry Fundamentals* **1976**, *15* (1), 59−64.

(5) Patel, N. C.; Teja, A. S. A new cubic equation of state for fluids and fluid mixtures. *Chem. Eng. Sci.* **1982**, *37* (3), 463−473.

(6) Lopez-Echeverry, J. S.; Reif-Acherman, S.; Araujo-Lopez, E. Peng-Robinson equation of state: 40 years through cubics. *Fluid Phase Equilib.* **2017**, *447*, 39−71.

(7) Bian, B.; Wang, Y.; Shi, J. Parameters for the PR and SRK equations of state. *Fluid phase equilibria* **1992**, *78*, 331−334.

(8) Abudour, A. M.; Mohammad, S. A.; Robinson, R. L., Jr; Gasem, K. A. Volume-translated Peng-Robinson equation of state for liquid densities of diverse binary mixtures. *Fluid Phase Equilib.* **2013**, *349*, 37−55.

(9) Ghoderao, P. N.; Dalvi, V. H.; Narayan, M. A five-parameter cubic equation of state for pure fluids and mixtures. *Chemical Engineering Science: X* **2019**, *3*, 100026.

(10) Wenzel, H.; Schmidt, G. A modified van der Waals equation of state for the representation of phase equilibria between solids, liquids and gases. *Fluid Phase Equilib.* **1980**, *5* (1−2), 3−17.

(11) Salim, P. H.; Trebble, M. A. Modelling of solid phases in thermodynamic calculations via translation of a cubic equation of state at the triple point. *Fluid phase equilibria* **1994**, *93*, 75−99.

(12) Yokozeki, A. Analytical equation of state for solid-liquid-vapor phases. *Int. J. Thermophys.* **2003**, *24* (3), 589−620.

(13) Lee, J. H.; Yoo, K.-P. Comments on "Analytic Equation of State for Solid-Liquid-Vapor Phases"(Int. J. Thermophys. 24, 589 (2003)). *Int. J. Thermophys.* **2011**, *32* (3), 553−558.

(14) Lee, J. H.; Shin, M. S.; Yoo, K.-P. Development of Single Insertion Probability for Equation of State Applicable to Three Phases of Matter. *Ind. Eng. Chem. Res.* **2011**, *50* (7), 4166−4176.

(15) Guevara-Rodriguez, F. d. J. A methodology to define the Cubic Equation of State of a simple fluid. *Fluid phase equilibria* **2011**, *307* (2), 190−196.

(16) Guevara-Rodríguez, F. d. J.; Romero-Martínez, A. An empirical extension for a generalized cubic equation of state, applied to a pure substance with small molecules. *Fluid Phase Equilib.* **2013**, *347*, 22−27.

(17) Jayanti, P. C.; Venkatarathnam, G. Identification of the phase of a substance from the derivatives of pressure, volume and temperature, without prior knowledge of saturation properties: Extension to solid phase. *Fluid Phase Equilib.* **2016**, *425*, 269−277.

(18) Stringari, P.; Campestrini, M.; Coquelet, C.; Arpentinier, P. An equation of state for solid-liquid-vapor equilibrium applied to gas processing and natural gas liquefaction. *Fluid Phase Equilib.* **2014**, *362*, 258−267.

(19) Marín-García, J. M.; Romero-Martínez, A.; Guevara-Rodriguez, F. d. J. Application of a non-cubic equation of state to predict the solid-liquid-vapor phase coexistences of pure alkanes. *Chem. Eng. Commun.* **2022**, *209*, 171−183.

(20) Setzmann, U.; Wagner, W. A new equation of state and tables of thermodynamic properties for methane covering the range from the melting line to 625 K at pressures up to 100 MPa. *Journal of Physical and Chemical reference data* **1991**, *20* (6), 1061−1155.

(21) *Quantifying Uncertainty in Analytical Measurement*, 3rd ed.; Ellison, S. L., Williams, A., Eds.; Eurachem/CITAC Guide, Vol. 4Eurachem/CITAC: Teddington, U.K., 2012. DOI: 10.25607/OBP-952

(22) Bücker, D.; Wagner, W. A reference equation of state for the thermodynamic properties of ethane for temperatures from the melting line to 675 K and pressures up to 900 MPa. *Journal of physical and chemical reference data* **2006**, *35* (1), 205−266.

(23) Lemmon, E. W.; McLinden, M. O.; Wagner, W. Thermodynamic properties of propane. III. A reference equation of state for temperatures from the melting line to 650 K and pressures up to 1000 MPa. *Journal of Chemical & Engineering Data* **2009**, *54* (12), 3141−3180.

(24) Younglove, B.; Ely, J. F. Thermophysical properties of fluids. II. Methane, ethane, propane, isobutane, and normal butane. *J. Phys. Chem. Ref. Data* **1987**, *16* (4), 577−798.
(25) Span, R.; Wagner, W. A new equation of state for carbon dioxide covering the fluid region from the triple-point temperature to 1100 K at pressures up to 800 MPa. *Journal of physical and chemical reference data* **1996**, *25* (6), 1509−1596.
(26) Clarke, E.; Glew, D. Deuterium and hydrogen sulfides: vapor pressures, molar volumes, and thermodynamic properties. *Can. J. Chem.* **1970**, *48* (5), 764−775.
(27) Sakoda, N.; Uematsu, M. A thermodynamic property model for fluid phase hydrogen sulfide. *Int. J. Thermophys.* **2004**, *25* (3), 709−737.
(28) Karan, K.; Heidemann, R. A.; Behie, L. A. Sulfur solubility in sour gas: predictions with an equation of state model. *Industrial & engineering chemistry research* **1998**, *37* (5), 1679−1684.
(29) Neumann, K. Dampfdruckmessungen an rhombischem und monoklinem Schwefel unterhalb des Schmelzpunktes. *Zeitschrift für Physikalische Chemie* **1934**, *171A* (1), 416−420.
(30) Ferreira, A.; Lobo, L. The low-pressure phase diagram of sulfur. *J. Chem. Thermodyn.* **2011**, *43* (2), 95−104.
(31) Kiran, E.; Sengers, J. M. H. L. FUTURE DIRECTIONS—A Summary of the Final Discussions. In *Supercritical Fluids*; Kiran, E., Sengers, J. M. H. L., Eds.; Springer, 1994; pp 761−771. DOI: 10.1007/978-94-015-8295-7_35.
(32) Zhang, R.; Gu, S.; Huang, L.; Zeng, D.; Li, T.; Zhang, G. Experimental study on the elemental sulfur solubility in sour gas mixtures. *Frontiers in Earth Science* **2021**, *9*, 931.
(33) Heidemann, R. A.; Phoenix, A. V.; Karan, K.; Behie, L. A. A chemical equilibrium equation of state model for elemental sulfur and sulfur-containing fluids. *Industrial & engineering chemistry research* **2001**, *40* (9), 2160−2167.
(34) Li, C.; Liu, G.; Peng, Y. Predicting sulfur solubility in hydrogen sulfide, carbon dioxide, and methane with an improved thermodynamic model. *RSC Adv.* **2018**, *8* (29), 16069−16081.

https://doi.org/10.1021/acsomega.1c06142
ACS Omega 2022, 7, 9322−9332